

IU/NTC 96-03

# Relativistic Mean-Field Theory and the High-Density Nuclear Equation of State

Horst Müller and Brian D. Serot

*Physics Department and Nuclear Theory Center*

*Indiana University, Bloomington, Indiana 47405*

(November 26, 2024)

## Abstract

The properties of high-density nuclear and neutron matter are studied using a relativistic mean-field approximation to the nuclear matter energy functional. Based on ideas of effective field theory, nonlinear interactions between the fields are introduced to parametrize the density dependence of the energy functional. Various types of nonlinearities involving scalar-isoscalar ( $\sigma$ ), vector-isoscalar ( $\omega$ ), and vector-iso vector ( $\rho$ ) fields are studied. After calibrating the model parameters at equilibrium nuclear matter density, the model and parameter dependence of the resulting equation of state is examined in the neutron-rich and high-density regime. It is possible to build different models that reproduce the same observed properties at normal nuclear densities, but which yield maximum neutron star masses that differ by more than one solar mass. Implications for the existence of kaon condensates or quark cores in neutron stars are discussed.

Typeset using REV<sub>T</sub>EX

## I. INTRODUCTION

Numerous calculations have established that relativistic mean-field models provide a realistic description of the bulk properties of finite nuclei and nuclear matter [1,2]. In addition to this successful low-energy phenomenology, these models are often extrapolated into regimes of high density and temperature to extract the nuclear equation of state (EOS), which is the basic ingredient in many astrophysical applications and in microscopic models of energetic nucleus–nucleus collisions.

Based on the original version of Walecka [3] and its extensions [4,5], relativistic mean-field models generally involve the interaction of Dirac nucleons with neutral scalar and vector mesons and with isovector  $\rho$  mesons. One of the key observations in their success is that to provide sufficient flexibility, nonlinear self-interactions for the scalar meson must be included [2,4,6–11]. Since these models were proposed to be renormalizable, the scalar self-interactions are limited to a quartic polynomial, and scalar–vector and vector–vector interactions are not allowed [12]. One of the motivations for renormalizability, as discussed in Walecka’s seminal paper, is that once the model parameters are calibrated to observed nuclear properties, one can extrapolate into regimes of high density or temperature without the appearance of new, unknown parameters.

An alternative approach is inspired by *effective* field theories, such as chiral perturbation theory [13,14], which successfully describes the low-energy phenomenology of hadronic Goldstone bosons [15,16]. Although a lagrangian usually serves as the starting point, the meson and baryon fields are no longer considered elementary, and the constraint of renormalizability is dropped. This has several important consequences. First, there is no reason to restrict meson self-interactions to a simple quartic polynomial in the scalar field; on the contrary, one should include all interaction terms that are consistent with the underlying symmetries of QCD. Second, since there are an infinite number of coupling constants, one must find suitable expansion parameters for the systems under consideration, and one must develop a systematic truncation scheme for the effective theory to have any predictive power. Third, extrapolation of calculated results into new regimes of the physical parameters becomes problematic, because the truncation scheme may break down, and predictions can become sensitive to unknown parameters.

Within the framework of effective field theory, mean-field models of nuclear structure and the EOS must be interpreted in a new context. One important observation is that near normal nuclear density, the mean scalar and vector fields (or nucleon self-energies), which we denote as  $\Phi$  and  $W$ , are large on nuclear energy scales but are small compared to the nucleon mass  $M$  and vary slowly in finite nuclei. This implies that the ratios  $\Phi/M$  and  $W/M$  and the gradients  $|\nabla\Phi|/M^2$  and  $|\nabla W|/M^2$  are useful expansion parameters. The assumption of “naturalness” in effective field theory is also important. Naturalness implies that the coefficients of the various terms in the lagrangian, when expressed in appropriate dimensionless form, should all be of order unity. When combined with meaningful expansion parameters, this means that one can anticipate the approximate magnitude of mean-field contributions to the energy (at least up to moderate nuclear densities) and thereby motivate a suitable truncation scheme; if the coefficients are natural, the omitted terms will be numerically

unimportant.<sup>1</sup> Naturalness also implies that one should include *all* possible terms (that is, those allowed by the symmetries) through a given order of truncation; it is *unnatural* for some coefficients to vanish without a relevant symmetry argument.

From this point of view, it is difficult to justify nuclear mean-field models that include only scalar self-interactions [4,6,7,10], and recently, generalizations that also include quartic self-interactions for the neutral vector meson have been discussed [9,19,20]. Moreover, a new analysis involving all meson self-interactions through fourth order in the isoscalar scalar and vector fields has been performed [21]. These extensions give rise to additional model parameters (coupling constants) that must be constrained by calibrating to observed nuclear properties. For the truncation at fourth order to be sensible, the parameters so obtained should exhibit naturalness.

Although it is possible to discuss effective hadronic field theory from the point of view of a lagrangian, as above, the expansion in powers of the mean fields is a low-density expansion, and it is hard to justify the neglect of many-body corrections, which are known to be relevant in nuclear structure and in the EOS. Alternatively, one can consider this expansion at the level of an energy functional or effective action [21]. In such a formulation of the relativistic nuclear many-body problem, the central object is an energy functional of scalar and vector densities (or more generally, vector four-currents) [22–24]. Extremization of the functional gives rise to Dirac equations for occupied orbitals with *local* scalar and vector potentials, not only in the Hartree approximation, but in the general case as well. Rather than work solely with the densities, one can introduce auxiliary variables corresponding to the local potentials, so that the functional depends also on mean meson fields. The resulting field equations have the same form as in a Dirac–Hartree calculation [21], but correlation effects can be included, *if* the proper energy functional can be found. This procedure is analogous to the well-known Kohn–Sham [25] approach in density-functional theory, with the local meson fields playing the role of (relativistic) Kohn–Sham potentials; by introducing nonlinear couplings between these fields, one can implicitly include additional density dependence in the potentials. Thus the nonlinear meson interaction terms simulate more complicated physics, such as one- and two-pion exchange, or vacuum-loop corrections, which might be calculated directly in a more microscopic many-body approach [20,24]. The fields (and their gradients) again serve as useful expansion parameters at moderate density, so the nonlinear interaction terms can be truncated, leaving a finite number of unknown couplings.

Rather than focus on the calculation of the nonlinear couplings from an underlying effective lagrangian, we wish to concentrate instead on how well the energy functional can be calibrated by fitting the couplings to observed nuclear properties, and on the limitations on the extrapolation of the resulting EOS into the high-density regime. In general, even with a significant truncation, the number of unknown couplings exceeds the number of normalization conditions, which we take to be five properties of infinite nuclear matter: the equilibrium density and binding energy ( $\rho_0, -e_0$ ), the nucleon effective (or Dirac) mass at equilibrium ( $M_0^*$ ), the compression modulus ( $K_0$ ), and the bulk symmetry energy ( $a_4$ ). (Experience has shown that an accurate reproduction of these five properties leads to realistic

---

<sup>1</sup>It has also been shown recently that the naturalness assumption is consistent with dimensional counting in chiral perturbation theory [17,18].

results when the calculations are extended to finite nuclei [6,7,10,11,21].) Thus families of models can be generated which describe exactly the same nuclear matter properties at equilibrium [19]. We then investigate the differences in the high-density EOS predicted by models within a given family. This question is important for astrophysical applications, particularly in the study of neutron stars; it will be difficult to deduce the existence of “exotic” neutron-star structure (for example, hyperonic matter, kaon condensates, or quark cores) unless the EOS of the more mundane components (neutrons, protons, and electrons) is well constrained.

If our truncation of the energy functional is motivated by low-density behavior, why should we have any confidence at all in a high-density extrapolation? This is indeed the crucial question, and we are not attempting here to justify such an extrapolation; we are merely recognizing that this procedure is often used in neutron-star calculations, even recent ones, without any mention of the implicit assumptions about the absence of additional contributions at high density [26–32]. We therefore feel it is timely to investigate quantitatively the uncertainties in the extrapolated equation of state.

We begin the theoretical analysis with a model that contains meson–meson and meson self-interactions described by an *arbitrary* finite polynomial in the fields. We find that both the asymptotic (high-density) limit of the EOS and the approach to this limit (*i.e.*, the “stiffness”) are model dependent. In particular, one can construct models with the *same* equilibrium nuclear matter properties that yield high-density equations of state ranging all the way from the causal limit ( $p = \mathcal{E}$ ) to one that resembles a free relativistic gas ( $p = \mathcal{E}/3$ ) [9,19]. (Here  $p$  is the pressure and  $\mathcal{E}$  is the energy density.)

As an explicit example, we consider a model that includes self-interactions for the isoscalar scalar and vector mesons and for the  $\rho$  meson up to fourth order in the fields. To our knowledge, this is the first time nonlinear terms in the  $\rho$  meson mean field have been included. (Note that the  $\rho$  field enters here as an *effective* field whose purpose is to parametrize the isospin dependence; thus, fundamental questions about causal propagation [33,34] and spin mixing [35] are not relevant.) To provide a quantitative measure of the variations in the EOS, we compute neutron star masses, which turn out to be sensitive to the model types and to changes in the parametrizations, *even for models that reproduce the same equilibrium nuclear matter properties*. In some cases, variations in the calculated maximum mass are more than one solar mass.

These results lead us to two basic conclusions. First, existing methods for calibration of the EOS at normal density are *not* sufficient to provide a satisfactory extrapolation into the density regime relevant for neutron stars. The basic problem rests with the quartic neutral vector meson ( $\omega$ ) interaction, which produces major modifications in the high-density behavior. We discuss the existing situation regarding the specification of this term and prospects for improved calibration. Second, we find that if the quartic  $\omega$  term can be accurately determined, additional higher-order terms (and the quartic  $\rho$  term) produce relatively minor changes in the neutron star mass. This occurs because the  $W^4$  term softens the high-density EOS so completely that additional interactions have little effect, at least in the density regime relevant for neutron stars.

These conclusions have important implications, because the contributions to the EOS from the neutrons and protons are commonly believed to be the best understood part of the physical input necessary to describe a dense stellar object. Without well-constrained results

from this part of the EOS, it will be impossible to determine the importance of additional dynamics, for example, the transition from nuclear matter to quark matter in the interiors of neutron stars [36,37,27], or the role of strangeness in the form of hyperons [38,39] or a kaon condensate [40]. As an example of how uncertainties in the basic nuclear EOS can influence these interesting effects, we study the transition from hadronic matter to quark matter using a simple model [37,1] and show the possible variations in the results.

The outline of this paper is as follows: In Sec. II, we present the general model, which involves an arbitrary number of nonlinear meson interactions, and derive the EOS. Based on this general model, Section III is devoted to the high-density limit of the EOS. In Sec. IV, we apply our model to neutron stars. For the quantitative analysis, we initially include self-interactions up to fourth order in the  $\rho$  and  $\omega$  fields and then investigate the consequences of sixth-order and eighth-order  $\omega$  self-interactions. We also briefly discuss the parameter and model dependence of the transition to quark matter in the central region of the star. Section V contains a short summary and our conclusions.

## II. THE NUCLEAR EQUATION OF STATE

We describe the nuclear equation of state using a relativistic approach involving valence Dirac nucleons and effective mesonic degrees of freedom, which are taken to be neutral scalar and vector fields, plus the isovector  $\rho$  meson field. Rather than focus directly on a lagrangian, we consider instead as a starting point an *effective action*

$$\Gamma = \Gamma[\phi, V_\mu, \mathbf{b}_\mu] , \quad (1)$$

which is a functional of the meson fields denoted by  $\phi$ ,  $V_\mu$ , and  $\mathbf{b}_\mu$  for the scalar, vector-isoscalar, and vector- isovector field, respectively. In principle, this functional can be calculated in a many-body approach based on a Lagrangian for the nucleon–nucleon interaction, or its general form might be obtained from an underlying theory. Here we will be satisfied to parametrize the effective action, calibrate it as accurately as we can to observed nuclear properties, and then examine the predicted high-density equation of state.

The effective action is related to the thermodynamic potential  $\Omega$  [41] by

$$i\beta\Omega = \Gamma[\phi, V_\mu, \mathbf{b}_\mu] , \quad (2)$$

where the fields are determined by the general thermodynamic principle that they should make  $\Omega$  stationary:

$$\frac{\partial\Gamma}{\partial\phi} = \frac{\partial\Gamma}{\partial V_\mu} = \frac{\partial\Gamma}{\partial\mathbf{b}_\mu} = 0 . \quad (3)$$

A basic property of the functional is that it reflects the underlying symmetries [42]. Thus, if we assume that the system possesses two conserved charges, namely, baryon number  $B$  and the third component of total isospin  $I_3$ , this gives rise to two chemical potentials  $\mu$  and  $\nu$ :

$$\Omega \equiv \Omega(\beta, \mu, \nu) , \quad (4)$$

with

$$B = \int d^3x \rho = -\frac{\partial \Omega}{\partial \mu} , \quad (5)$$

$$I_3 = \frac{1}{2} \int d^3x \rho_3 = -\frac{\partial \Omega}{\partial \nu} , \quad (6)$$

$\beta$  the inverse temperature, and  $\rho_3 \equiv \rho_p - \rho_n$ . Note that the fields can be held fixed in evaluating the partial derivatives in Eqs. (5) and (6) by virtue of the extremization conditions (3).

In the field theoretical context [43], one can show that the effective action can be expanded as a power series in gradients of the fields. Thus, after taking the zero-temperature limit, one usually writes

$$\Gamma[\phi, V_\mu, \mathbf{b}_\mu] = \int d^4x \left[ -\mathcal{V}_{\text{eff}}(\phi, V_\mu, \mathbf{b}_\mu) + \mathcal{Z}(\phi, V_\mu, \mathbf{b}_\mu, \partial_\nu \phi, \partial_\nu V_\mu, \partial_\nu \mathbf{b}_\mu) \right] , \quad (7)$$

where the second term vanishes in a uniform system, and the dependence on the chemical potentials has been suppressed. For the effective potential, we make the following *Ansatz*:

$$\begin{aligned} \mathcal{V}_{\text{eff}}(\phi, V_\mu, \mathbf{b}_\mu; \mu, \nu) = & \frac{1}{2} m_s^2 \phi^2 - \frac{1}{2} m_v^2 V_\mu V^\mu - \frac{1}{2} m_\rho^2 \mathbf{b}_\mu \cdot \mathbf{b}^\mu \\ & + i \text{tr} \ln Z_\psi(\mu, \nu) - i \text{tr} \ln Z_\psi(0, 0) \\ & + \Delta \mathcal{V}(\phi, V_\mu V^\mu, \mathbf{b}_\nu \cdot \mathbf{b}^\nu; \mu, \nu) , \end{aligned} \quad (8)$$

with a nonlinear potential

$$\Delta \mathcal{V}(\phi, V_\mu V^\mu, \mathbf{b}_\nu \cdot \mathbf{b}^\nu; \mu, \nu) \equiv - \sum_{i,j,k} a_{ijk}(\mu, \nu) \phi^i (V_\mu V^\mu)^j (\mathbf{b}_\nu \cdot \mathbf{b}^\nu)^k \quad (9)$$

that contains at least three powers of the fields:  $i + 2j + 2k \geq 3$ . The fermionic contributions are represented by a one-body term  $\text{tr} \ln Z_\psi$  (with the appropriate zero-density subtraction [44]) and by terms where the fermions have been “integrated out”, which results in a (generally nonanalytic) dependence of the mesonic coefficients  $a_{ijk}$  on the chemical potentials  $\mu$  and  $\nu$ . There will also be contributions to the  $a_{ijk}$  that are independent of the chemical potentials; these arise from integrating out heavy degrees of freedom and vacuum loops. Thus  $\mathcal{V}_{\text{eff}}$  contains explicit contributions only from valence nucleons and classical meson fields.

The fermionic part  $\text{tr} \ln Z_\psi$  is obtained by evaluating the trace of the kernel

$$K(\mu, \nu) = (i\partial^\mu - g_v V^\mu - \frac{1}{2} g_\rho \boldsymbol{\tau} \cdot \mathbf{b}^\mu) \gamma_\mu + \mu \gamma^0 + \frac{1}{2} \nu \tau_3 \gamma^0 - (M - g_s \phi) \quad (10)$$

using Dirac wave functions calculated in the presence of static background fields. The subtraction removes contributions from negative-energy states, which are already included implicitly in the nonlinear parameters  $a_{ijk}$ . (See Ref. [44] for an analogous calculation.) The values of the fields are determined by extremization at the given values of  $\mu$  and  $\nu$ .

The potential of Eq. (8) represents an effective field theory for the interacting nucleons. Although the exact form of the effective potential is not known, we introduce the meson mean fields as relativistic Kohn–Sham potentials [25] and consider the valence nucleons moving in the resulting local fields. The nonlinear interactions of the fields generate implicit density dependence above and beyond that arising from the couplings in Eq. (10). Thus the

series in Eq. (9) can be interpreted as a Taylor series parametrization of the unknown part of the effective potential, which includes the effects of nucleon exchange and correlations, as well as contributions from other mesons and the quantum vacuum. (See the discussion in Refs. [21,44].)

Although the couplings  $a_{ijk}$  generally depend on the chemical potentials, experience with calculations for finite nuclei and nuclear matter, together with explicit computations of exchange and correlation corrections [45], implies that mean fields and *constant* couplings  $a_{ijk}$  provide an adequate (albeit approximate) parametrization of these many-body effects. Thus we consider the  $a_{ijk}$  as constants in the sequel and leave the study of their dependence on  $\mu$  and  $\nu$  as a topic for future investigation. Moreover, at low densities and temperatures, the mean meson fields are small compared to the nucleon mass, and so provide useful expansion parameters [21]. Thus, in practice, the series in Eq. (9) can be truncated at some reasonable order, and the relevant question in this paper is how far one can extrapolate the truncated potential into the high-density regime.

In principle, the unknown coefficients (coupling constants) can be constrained by imposing chiral symmetry and other symmetries of the underlying QCD, such as broken scale invariance. (Lorentz covariance and isospin symmetry are already incorporated explicitly.<sup>2</sup>) As has been discussed recently, however [11,21], if one assumes a *nonlinear* realization of the chiral symmetry for the pions and nucleons [46], the meson interaction terms are essentially unconstrained.<sup>3</sup> We therefore take the couplings as free model parameters in our approach. Obviously, an infinite number of normalization conditions is generally needed to fix their values. Since this is not feasible in practice, we terminate the summation at the finite values  $i_{\max}$ ,  $j_{\max}$ , and  $k_{\max}$ .

According to Eq. (3), the thermodynamic potential  $\Omega$  must be stationary with respect to changes in the fields for fixed values of the proton and neutron chemical potentials

$$\mu_p \equiv \mu + \frac{\nu}{2} = (k_{Fp}^2 + M^{*2})^{1/2} + W + \frac{1}{2}R, \quad (11)$$

$$\mu_n \equiv \mu - \frac{\nu}{2} = (k_{Fn}^2 + M^{*2})^{1/2} + W - \frac{1}{2}R. \quad (12)$$

Here, following Bodmer [19], we define the scaled meson fields  $\Phi \equiv g_s \phi$ ,  $W \equiv g_v V_0$ , and  $R \equiv g_\rho b_0$ , with  $b_0$  the timelike, neutral part of the  $\rho$  meson field; the effective nucleon mass is  $M^* \equiv M - \Phi$ . (We work in the rest frame of the infinite matter, where the spatial parts of the vector fields vanish.) The Fermi momenta for protons ( $k_{Fp}$ ) and neutrons ( $k_{Fn}$ ) are related to the conserved baryon density

$$\rho = \frac{1}{3\pi^2} (k_{Fp}^3 + k_{Fn}^3) \quad (13)$$

---

<sup>2</sup>Note that since the energy functional is an effective functional, we presently know of no reason to exclude terms that explicitly contain the medium four-velocity  $u^\mu$ , such as  $u^\mu V_\mu V^\nu V_\nu$ . This issue will be considered in a later publication.

<sup>3</sup>Broken scale invariance leads to restrictions on the purely scalar interactions, as shown in Refs. [47] and [44], but we will not consider these limitations here. As discussed in the next section, the details of the scalar dynamics do not play a major role in our analysis.

and isovector density

$$\rho_3 = \frac{1}{3\pi^2} (k_{\text{Fp}}^3 - k_{\text{Fn}}^3). \quad (14)$$

Using Eqs. (2), (5), and (6), together with relations (11) and (12) for the chemical potentials, it is straightforward to eliminate the chemical potentials in favor of the densities and to compute the pressure  $p$  and the energy density  $\mathcal{E} = -p + \mu\rho + \frac{1}{2}\nu\rho_3$ :

$$\begin{aligned} p &= \frac{1}{3\pi^2} \int_0^{k_{\text{Fp}}} dk \frac{k^4}{(k^2 + M^{*2})^{1/2}} + \frac{1}{3\pi^2} \int_0^{k_{\text{Fn}}} dk \frac{k^4}{(k^2 + M^{*2})^{1/2}} \\ &+ \frac{1}{2c_v^2} W^2 + \frac{1}{2c_\rho^2} R^2 - \frac{1}{2c_s^2} \Phi^2 + \sum_{i,j,k} \bar{a}_{ijk} \Phi^i W^{2j} R^{2k}, \end{aligned} \quad (15)$$

$$\begin{aligned} \mathcal{E} &= \frac{1}{\pi^2} \int_0^{k_{\text{Fp}}} dk k^2 (k^2 + M^{*2})^{1/2} + \frac{1}{\pi^2} \int_0^{k_{\text{Fn}}} dk k^2 (k^2 + M^{*2})^{1/2} \\ &+ W\rho + \frac{1}{2} R\rho_3 - \frac{1}{2c_v^2} W^2 - \frac{1}{2c_\rho^2} R^2 + \frac{1}{2c_s^2} \Phi^2 - \sum_{i,j,k} \bar{a}_{ijk} \Phi^i W^{2j} R^{2k}. \end{aligned} \quad (16)$$

Here the ratios  $c_i^2 = g_i^2/m_i^2$  and  $\bar{a}_{ijk} \equiv a_{ijk}/(g_s^i g_v^{2j} g_\rho^{2k})$  have been introduced for convenience.

As noted earlier, the pressure in Eq. (15) and the energy density in Eq. (16) also contain vacuum contributions arising from the partition function of the nucleons. However, at least at the one-baryon-loop level, these vacuum terms can be absorbed in the definition of the nonlinear couplings in Eq. (9) [44], and thus we include explicitly only the contributions from valence nucleons.

At zero temperature, the stationarity conditions of Eq. (3) with fixed chemical potentials are equivalent to an extremization of the energy at fixed baryon and isovector density. This leads to the self-consistency equations

$$\frac{1}{c_s^2} \Phi - \sum_{i,j,k} i \bar{a}_{ijk} \Phi^{i-1} W^{2j} R^{2k} = \rho_s, \quad (17)$$

$$\frac{1}{c_v^2} W + \sum_{i,j,k} 2j \bar{a}_{ijk} \Phi^i W^{2j-1} R^{2k} = \rho, \quad (18)$$

$$\frac{1}{c_\rho^2} R + \sum_{i,j,k} 2k \bar{a}_{ijk} \Phi^i W^{2j} R^{2k-1} = \frac{1}{2} \rho_3, \quad (19)$$

where the scalar density is given by

$$\rho_s = \frac{M^*}{\pi^2} \int_0^{k_{\text{Fp}}} dk \frac{k^2}{(k^2 + M^{*2})^{1/2}} + \frac{M^*}{\pi^2} \int_0^{k_{\text{Fn}}} dk \frac{k^2}{(k^2 + M^{*2})^{1/2}}. \quad (20)$$

Because of the factor of 1/2 on the right-hand side of Eq. (19), it follows that the relevant expansion parameters for the energy density are  $\Phi/M$ ,  $W/M$ , and  $2R/M$ . Moreover, by dividing  $\mathcal{E}$  by  $M^4$  and expressing the result in terms of these expansion parameters, one can identify the scaled couplings that should all be of roughly the same size if they are “natural”, namely,

$$\frac{1}{2c_s^2 M^2}, \quad \frac{1}{2c_v^2 M^2}, \quad \frac{1}{8c_\rho^2 M^2}, \quad \text{and} \quad \frac{\bar{a}_{ijk} M^{i+2j+2k-4}}{2^{2k}}.$$

### III. THE HIGH-DENSITY LIMIT

The coupling constants  $c_v^2$ ,  $c_s^2$ ,  $c_\rho^2$ , and  $\bar{a}_{ijk}$  in Eqs. (15) and (16) enter as unknown model parameters. According to the generally accepted procedure, these parameters will be chosen to reproduce the properties of nuclear matter near equilibrium. The basic ingredient in many astrophysical problems, *e.g.*, neutron-star calculations, is the EOS

$$p = p(\mathcal{E}) , \quad (21)$$

which is then extrapolated into the neutron-rich and high-density regime. Anticipating the results of the next section, one can expect that different parameter sets that lead to identical equilibrium properties produce qualitatively similar equations of state at low densities. The relevant question is whether this qualitatively similar behavior persists at high densities, particularly in the regime important for neutron stars. As a first step in this direction, we investigate the high-density limit of the EOS generated by the model introduced in the previous section.

To make the discussion more transparent, we focus here on pure neutron matter ( $k_{Fp} = 0$ ,  $k_{Fn} \equiv k_F$ ), although nuclear matter in  $\beta$ -decay equilibrium with a finite proton to neutron ratio is necessary to achieve accurate results for maximum neutron star masses. We will return to this issue in the next section.

It is clear that a sufficiently large number of couplings introduces a high degree of flexibility. Due to the nonlinearity of the problem, not all families of parameter sets lead to physically acceptable results, which provides one way to restrict the parameter space. Classes of models can be ruled out if basic physical requirements are violated. For example, one certainly requires that the pressure  $p$  be a smooth function of the energy density  $\mathcal{E}$ . Moreover, it is necessary that the speed of (first) sound  $c_1$  respect causality and also be real, to ensure stability. That is,

$$0 \leq c_1^2 = \frac{\partial p}{\partial \mathcal{E}} \leq 1 .$$

In addition to these general principles, we require a positive and bounded value of the nucleon effective mass, *i.e.*,

$$0 \leq M^* \leq M . \quad (22)$$

This is motivated by the expectation that physically reasonable models will demonstrate some degree of chiral-symmetry restoration at finite density, leading to a reduction in the nucleon mass, with the most extreme situation corresponding to total restoration of the symmetry. The consequences of Eq. (22) will become more transparent in the following.

By specializing the formalism of the preceding section to pure neutron matter and by using the self-consistency equations (17)–(19), the pressure and energy density can be expressed as

$$\begin{aligned} p &\equiv p_0(k_F, M^*) + \Delta p(\Phi, W, R) \\ &= \frac{1}{3\pi^2} \int_0^{k_F} dk \frac{k^4}{(k^2 + M^{*2})^{1/2}} \\ &\quad + \frac{1}{2c_v^2} W^2 + \frac{1}{2c_\rho^2} R^2 - \frac{1}{2c_s^2} \Phi^2 + \sum_{i,j,k} \bar{a}_{ijk} \Phi^i W^{2j} R^{2k} , \end{aligned} \quad (23)$$

$$\begin{aligned}
\mathcal{E} &\equiv \mathcal{E}_0(k_F, M^*) + \Delta\mathcal{E}(\Phi, W, R) \\
&= \frac{1}{\pi^2} \int_0^{k_F} dk k^2 (k^2 + M^{*2})^{1/2} \\
&\quad + \frac{1}{2c_v^2} W^2 + \frac{1}{2c_\rho^2} R^2 + \frac{1}{2c_s^2} \Phi^2 + \sum_{i,j,k} (2j + 2k - 1) \bar{a}_{ijk} \Phi^i W^{2j} R^{2k} ,
\end{aligned} \tag{24}$$

where  $p_0$  and  $\mathcal{E}_0$  denote the results for a relativistic, noninteracting gas of spin-1/2 baryons with mass  $M^*$ . Note that these expressions include, as a special case, models where only the  $\bar{a}_{0jk}$  are nonzero, so that there are no scalar–vector couplings. Moreover, the isovector density in Eq. (19) is replaced by

$$\rho_3 = -\rho = -\frac{1}{3\pi^2} k_F^3 . \tag{25}$$

At high densities, the left-hand sides of the self-consistency equations (18) and (19) must grow linearly in  $\rho$ , and thus we start with the *Ansatz*

$$\lim_{\rho \rightarrow \infty} W = w_0 \rho^\alpha \quad , \quad \lim_{\rho \rightarrow \infty} R = r_0 \rho^\beta , \tag{26}$$

where  $0 < \alpha, \beta \leq 1$ ,  $w_0 > 0$ , and  $r_0 < 0$ . Since we assume that the effective mass is bounded, we can replace the scalar field by the limit

$$\Phi_\infty \equiv \lim_{\rho \rightarrow \infty} (M - M^*) \leq M . \tag{27}$$

To fulfill the resulting self-consistency equations:

$$\frac{1}{c_v^2} W + \sum_{i,j,k} 2j \bar{a}_{ijk} \Phi_\infty^i W^{2j-1} R^{2k} = \rho , \tag{28}$$

$$\frac{1}{c_\rho^2} R + \sum_{i,j,k} 2k \bar{a}_{ijk} \Phi_\infty^i W^{2j} R^{2k-1} = \frac{1}{2} \rho_3 = -\frac{1}{2} \rho , \tag{29}$$

there must be integers  $(j_m, k_m)$  and  $(j'_m, k'_m)$  with

$$(2j_m - 1)\alpha + 2k_m\beta = 1 > (2j - 1)\alpha + 2k\beta \quad \text{for all } j \neq j_m, k \neq k_m , \tag{30}$$

$$2j'_m\alpha + (2k'_m - 1)\beta = 1 > 2j\alpha + (2k - 1)\beta \quad \text{for all } j \neq j'_m, k \neq k'_m . \tag{31}$$

(This assumes that only one term in each sum produces the leading asymptotic behavior; if this actually happens for more than one term in a sum, the conclusions below are unchanged.) Using

$$\lim_{\rho \rightarrow \infty} p_0 = \frac{(3\pi^2)^{1/3}}{4} \rho^{4/3} + O(\rho^{2/3}) \quad , \quad \lim_{\rho \rightarrow \infty} \mathcal{E}_0 = \frac{3(3\pi^2)^{1/3}}{4} \rho^{4/3} + O(\rho^{2/3}) , \tag{32}$$

the leading contributions to the pressure and the energy density are found to be

$$\begin{aligned} \lim_{\rho \rightarrow \infty} p &= \frac{(3\pi^2)^{1/3}}{4} \rho^{4/3} + \frac{1}{2c_v^2} w_0^2 \rho^{2\alpha} + \frac{1}{2c_\rho^2} r_0^2 \rho^{2\beta} \\ &\quad + w_0^{2j_m} r_0^{2k_m} \rho^{1+\alpha} \sum_i \bar{a}_{ij_m k_m} \Phi_\infty^i + w_0^{2j'_m} r_0^{2k'_m} \rho^{1+\beta} \sum_i \bar{a}_{ij'_m k'_m} \Phi_\infty^i , \end{aligned} \quad (33)$$

$$\begin{aligned} \lim_{\rho \rightarrow \infty} \mathcal{E} &= \frac{3(3\pi^2)^{1/3}}{4} \rho^{4/3} + \frac{1}{2c_v^2} w_0^2 \rho^{2\alpha} + \frac{1}{2c_\rho^2} r_0^2 \rho^{2\beta} \\ &\quad + w_0^{2j_m} r_0^{2k_m} \rho^{1+\alpha} (2j_m + 2k_m - 1) \sum_i \bar{a}_{ij_m k_m} \Phi_\infty^i \\ &\quad + w_0^{2j'_m} r_0^{2k'_m} \rho^{1+\beta} (2j'_m + 2k'_m - 1) \sum_i \bar{a}_{ij'_m k'_m} \Phi_\infty^i . \end{aligned} \quad (34)$$

To this point, the discussion is rather general. To make the conclusions more concrete, we discuss two distinct situations separately:

1. No coupling between  $W$  and  $R$ .

In this special case, the asymptotic behavior of the fields is governed by their highest powers in the potential (9). From Eqs. (30) and (31), we obtain

$$\alpha = \frac{1}{2j_{\max} - 1} \quad , \quad \beta = \frac{1}{2k_{\max} - 1} .$$

For  $j_{\max} = 1, k_{\max} \geq 1$  or  $j_{\max} \geq 1, k_{\max} = 1$ , the quadratic terms dominate the right-hand sides of Eqs. (33) and (34), so that

$$\lim_{\rho \rightarrow \infty} \frac{1}{c_v^2} W^2 \propto \rho^2 \quad \text{or} \quad \lim_{\rho \rightarrow \infty} \frac{1}{c_\rho^2} R^2 \propto \rho^2 .$$

This case includes the original version of the Walecka model [3] and generates the limiting behavior

$$\lim_{\rho \rightarrow \infty} p = \mathcal{E} . \quad (35)$$

The sums in  $\Delta p$  and  $\Delta \mathcal{E}$  contribute to the leading order only if  $j_{\max} = 2, k_{\max} \geq 2$  or  $j_{\max} \geq 2, k_{\max} = 2$ . In this case, the quadratic terms can be neglected, and  $\Delta p$  and  $\Delta \mathcal{E}$  are of the same order as the contributions from the ideal-Fermi-gas terms. However, the factors in Eq. (34) conspire such that

$$\lim_{\rho \rightarrow \infty} \Delta p = \frac{1}{3} \Delta \mathcal{E} , \quad (36)$$

and the functional form of the limiting EOS resembles that of an ideal Fermi gas:

$$\lim_{\rho \rightarrow \infty} p = \frac{1}{3} \mathcal{E} . \quad (37)$$

In the remaining cases ( $j_{\max} > 2, k_{\max} > 2$ ), the dominant contributions arise solely from  $p_0$  and  $\mathcal{E}_0$ , which also leads to Eq. (37). Note here the importance of Eq. (22), which implies that in the high-density limit,  $M^*$  becomes negligible, at least to leading order.

2. At least one coupling between  $W$  and  $R$ .

From Eqs (30) and (31), it follows directly that

$$\alpha \leq \frac{1}{3} \quad \text{and} \quad \beta \leq \frac{1}{3}.$$

The quadratic contributions in the fields are negligible, and  $\Delta p$  and  $\Delta \mathcal{E}$  contribute to the leading term only if  $\alpha = \beta = 1/3$ , where again Eq. (36) holds. In any event, this leads to the limit of Eq. (37).

To summarize, we conclude that the high-density limit of the EOS is strongly influenced by nonlinear meson–meson interactions, which agrees with the conclusion of Bodmer and Price [9,19]. The limit in Eq. (35) obtained in the original version of the Walecka model [3] is a special case; in the more general situation, the nuclear matter EOS approaches that of an ideal Fermi gas, given by Eq. (37). We will show in the next section that these two limits can be achieved using different models with parameter sets that reproduce the same equilibrium properties of nuclear matter.

#### IV. CONSEQUENCES FOR NEUTRON STARS

The high-density limit of the EOS and the way in which the matter approaches the asymptotic regime have important consequences in neutron star calculations. The masses and radii of stars are sensitive to the stiffness of the EOS, thus providing a quantitative measure for studying the impact of the nonlinear interaction terms in Eq. (9).

To be specific, it is necessary to choose an explicit potential, and we begin with the form

$$\sum_{i,j,k} a_{ijk} \phi^i (V_\mu V^\mu)^j (\mathbf{b}_\mu \cdot \mathbf{b}^\mu)^k = -\frac{\kappa}{3!} \phi^3 - \frac{\lambda}{4!} \phi^4 + \frac{\zeta}{4!} g_v^4 (V_\mu V^\mu)^2 + \frac{\xi}{4!} g_\rho^4 (\mathbf{b}_\mu \cdot \mathbf{b}^\mu)^2, \quad (38)$$

which includes a subset of the meson self-interactions up to fourth order in the fields. As discussed in the Introduction, setting some of the allowed cubic and quartic couplings to zero is “unnatural”, but as we will discover, the model defined by Eq. (38) is already general enough to produce significant differences in predicted neutron star masses, and restoring the omitted couplings will lead to even more variation in the results. Moreover, the present model can be related to the most common models discussed in the literature, and it generalizes them to include a nonlinear isovector interaction. The motivation for adding the quartic rho-meson term is that one expects this coupling to be essentially unconstrained by normal nuclear observables, where the neutron–proton asymmetry is low, but it may have significant impact on the neutron-rich matter in neutron stars. As noted earlier, since the meson fields are effective (Kohn–Sham) potentials, we are not concerned here with their elementary excitations, and considerations of causality [33,34] are unimportant.

In nuclear matter calculations, this model contains seven free parameters. The polynomial in Eq. (38) contains four couplings that we may write as  $\bar{\kappa} \equiv \kappa/g_s^3$ ,  $\bar{\lambda} \equiv \lambda/g_s^4$ ,  $\zeta$ , and  $\xi$ ; in addition, values for the three ratios  $c_i^2 = g_i^2/m_i^2$  ( $i = s, v, \rho$ ) are needed. Five of the seven parameters can be chosen to reproduce the equilibrium properties of symmetric nuclear matter, which we take as the equilibrium density and binding energy  $(\rho_0, -e_0)$ , the

nucleon effective (or Dirac) mass at equilibrium ( $M_0^*$ ), the compression modulus ( $K_0$ ), and the bulk symmetry energy ( $a_4$ ). The first three of these are tightly constrained [11], whereas the latter two are not. In principle, the sensitivity of the high-density EOS to reasonable variations in  $K_0$  and  $a_4$  could be examined, but for simplicity, we keep their values fixed in most of our calculations. The “standard” set of equilibrium properties used here are listed in Table I; these are motivated by successful descriptions of bulk and single-particle nuclear properties [11,44,21]. The nucleon mass is fixed at its empirical value ( $M = 939$  MeV).

Our primary goal is to study the influence of the nonlinear vector-meson interactions on neutron star masses. Since there are more free couplings than normalization conditions, we proceed as follows: We choose values for the couplings  $\zeta$  and  $\xi$  and determine the remaining couplings by requiring that they reproduce the desired equilibrium properties. This is achieved by solving a set of transcendental equations that relate the parameters directly to the nuclear matter properties [19,21]. Although we have no specific guidance on the allowed values of  $\zeta$  and  $\xi$ , we rely on the assumption of naturalness, and based on the discussion at the end of Sec. II, we observe that the following parameter combinations should all be of roughly equal size:

$$\frac{1}{2c_s^2 M^2}, \quad \frac{1}{2c_v^2 M^2}, \quad \frac{1}{8c_\rho^2 M^2}, \quad \frac{\bar{\kappa}}{6M}, \quad \frac{\bar{\lambda}}{24}, \quad \frac{\zeta}{24}, \quad \text{and} \quad \frac{\xi}{384}.$$

Typical values for the first three parameters are between 0.001 and 0.002, so that the natural values of  $\zeta$  and  $\xi$  are roughly limited to  $0 \leq \zeta \lesssim 0.06$  and  $0 \leq \xi \lesssim 1.0$ . (To avoid abnormal solutions of the vector field equations, *i.e.*, those with finite mean fields at zero density,  $\zeta$  and  $\xi$  must be positive.<sup>4</sup>) We will include results for vanishing  $\zeta$  and  $\xi$ , which are in a strict sense unnatural, in order to make contact with earlier calculations. For a more thorough discussion of naturalness and its implications, see Ref. [21].

Using the notation of Sec. II, the self-consistency equations (17)–(19) can be written as

$$\frac{1}{c_s^2} \Phi + \frac{\bar{\kappa}}{2} \Phi^2 + \frac{\bar{\lambda}}{6} \Phi^3 = \rho_s, \quad (39)$$

$$W \left( \frac{1}{c_v^2} + \frac{\zeta}{6} W^2 \right) = \rho, \quad (40)$$

$$R \left( \frac{1}{c_\rho^2} + \frac{\xi}{6} R^2 \right) = \frac{1}{2} \rho_3 = -\frac{1}{2} \rho. \quad (41)$$

The expressions for the pressure and the energy density follow as

$$\begin{aligned} p = & \frac{1}{3\pi^2} \int_0^{k_F} dk \frac{k^4}{(k^2 + M^{*2})^{1/2}} \\ & + \frac{1}{2c_v^2} W^2 + \frac{\zeta}{24} W^4 + \frac{1}{2c_\rho^2} R^2 + \frac{\xi}{24} R^4 - \frac{1}{2c_s^2} \Phi^2 - \frac{\bar{\kappa}}{6} \Phi^3 - \frac{\bar{\lambda}}{24} \Phi^4, \end{aligned} \quad (42)$$

---

<sup>4</sup>Note that positive  $\zeta$  and  $\xi$  imply that the resulting nonlinear interactions are *attractive*. This constraint on the highest-order vector interactions appears to be general and explains why our earlier analysis finds that nonlinear interactions soften the equation of state.

$$\begin{aligned}\mathcal{E} = & \frac{1}{\pi^2} \int_0^{k_F} dk k^2 (k^2 + M^{*2})^{1/2} \\ & + \frac{1}{2c_v^2} W^2 + \frac{\zeta}{8} W^4 + \frac{1}{2c_\rho^2} R^2 + \frac{\xi}{8} R^4 + \frac{1}{2c_s^2} \Phi^2 + \frac{\bar{\kappa}}{6} \Phi^3 + \frac{\bar{\lambda}}{24} \Phi^4 .\end{aligned}\quad (43)$$

We begin our discussion with the model introduced by Bodmer and Price [9], which corresponds to  $\zeta = 0$ . According to the discussion in the preceding section, this model has the interesting feature that the high-density EOS of pure neutron matter approaches  $p = \mathcal{E}$ , while in symmetric matter, where the mean-field of the  $\rho$  meson vanishes, the EOS approaches the massless Fermi gas limit, given by Eq. (37). In Fig. 1, we show the binding energy curves for symmetric and pure neutron matter for different values of the nonlinear coupling  $\zeta$ . We emphasize that all parametrizations reproduce the same equilibrium properties listed in Table I.

At low densities, all the curves approach a common limit, because the nonlinear terms do not contribute at leading order in a low-density expansion. At higher densities, the softening of the EOS as  $\zeta$  increases is clearly visible, at least for symmetric matter. The softening in neutron matter is more apparent in Fig. 2. In the regime of intermediate density,  $200 \lesssim \mathcal{E} \lesssim 1000$  MeV/fm<sup>3</sup>, the EOS becomes softer with increasing values of  $\zeta$  [19]. To study the approach to the asymptotic limit, we examine the nonleading terms in the high-density expansion:

$$\lim_{\mathcal{E} \rightarrow \infty} p = \mathcal{E} - \frac{1}{6\pi^2} \left( \frac{72\pi^4}{4c_v^2 + c_\rho^2} \right)^{2/3} \mathcal{E}^{2/3} + O(\mathcal{E}^{1/3}) \quad \text{for } \zeta = 0 , \quad (44)$$

$$\lim_{\mathcal{E} \rightarrow \infty} p = \mathcal{E} - \frac{1}{6\pi^2} \left( \frac{72\pi^4}{c_\rho^2} \right)^{2/3} \left[ 1 + \left( \frac{2}{\pi^2 \zeta} \right)^{1/3} \right] \mathcal{E}^{2/3} + O(\mathcal{E}^{1/3}) \quad \text{for } \zeta \neq 0 , \quad (45)$$

which reveals two important features. First, the  $\zeta \neq 0$  results are *nonanalytic* in  $\zeta$ . Thus one cannot reproduce Eq. (44) by taking the  $\zeta \rightarrow 0$  limit of Eq. (45); at least as far as  $\zeta$  is concerned, the high-density expansion is essentially a strong coupling expansion. Second, we observe that the coefficient of the nonleading term is smaller for  $\zeta = 0$  for two reasons: the appearance of the isoscalar coupling  $c_v^2$  in the denominator and the absence of the multiplicative factor containing  $\zeta$ . (Note that  $c_\rho^2$  is independent of  $\zeta$ .) These two features produce a coefficient that is roughly an order of magnitude smaller for  $\zeta = 0$  than for  $\zeta \neq 0$ , which explains the relatively slow approach to the asymptotic limit in the latter case, as is evident from Fig. 2.

The consequences for neutron stars can be studied in Fig. 3, where the star masses are shown as a function of the central mass density  $\rho_c$ . As expected from Fig. 2, the maximum mass decreases with increasing  $\zeta$ . This decrease is substantial: from  $M_{\max} = 2.9 M_\odot$  for  $\zeta = 0$  to  $M_{\max} = 2.1 M_\odot$  for  $\zeta = 0.06$ , which is roughly 30%. The shifts in the maximum mass are most dramatic for small couplings; for larger couplings, the softening effects begin to saturate.

To understand this result, it is useful to identify the regime of energy density that is most important in determining the mass of the star. This regime can be deduced from Fig. 4, where we show the radial mass density distributions for several neutron stars, as well as the corresponding energy densities. Observe that most of the mass is generated at radii between

6 and 12 km, which corresponds to energy densities of several hundred MeV/fm<sup>3</sup>. As can be seen from Fig. 2, this includes the regime where the EOS is sensitive to  $\zeta$ , because this is where the  $W^4$  contribution to the EOS begins to become important. Note, however, that the contribution of the  $W^4$  term in this regime is still smaller than that of the  $W^2$  term; the quartic term does not begin to dominate until the energy density reaches several thousand MeV/fm<sup>3</sup>, as indicated by the coalescence of the dashed and dotted curves in Fig. 2.

We now return to the general form in Eq. (38) and allow nonlinear self-interactions of the  $\rho$  mesons. In contrast to the isoscalar coupling  $\zeta$ , the new quantity  $\xi$  does not enter in the calculation of our five “standard” equilibrium properties of nuclear matter, and the other parameters are determined independently. This is true even for the symmetry energy, because the new coupling  $\xi$  first appears at order  $(N-Z)^4$  in an expansion around symmetric nuclear matter. In principle,  $\xi$  could be constrained by fits to liquid-drop expansions of the energy, but in most such fits this parameter is set to zero. (We found only one nonzero value in the literature [48].) Thus, at present, contributions to the symmetry energy beyond terms of order  $(N-Z)^2$  are practically unconstrained.

Fig. 5 shows the binding energy of nuclear matter as a function of the proton fraction  $y$  for two different densities. The curves are calculated for various values of  $\xi$  with  $\zeta$  held fixed. For clarity, we plot the fractional shift in  $\mathcal{E}$  relative to its value with  $\xi = 0$ . At normal nuclear density, results for different  $\xi$  are virtually indistinguishable, but at high density, the curves differ by a few percent when the proton fraction becomes very small. This demonstrates that it is possible to generate families of models that reproduce identical properties of nuclear matter at low and normal densities, but which generate different predictions at high densities.

According to the analysis in the preceding section, the EOS asymptotically approaches the massless Fermi gas limit for both symmetric and neutron matter. The high-density expansion for neutron matter corresponding to Eq. (45) is

$$\lim_{\mathcal{E} \rightarrow \infty} p = \frac{1}{3} \mathcal{E} + \frac{2\pi}{3} \frac{\left[ \frac{1}{c_v^2} \left( \frac{2}{\pi^2 \zeta} \right)^{2/3} + \frac{1}{c_\rho^2} \left( \frac{1}{\pi^2 \xi} \right)^{2/3} \right]}{\left[ 1 + \left( \frac{2}{\pi^2 \zeta} \right)^{1/3} + \left( \frac{1}{\pi^2 \xi} \right)^{1/3} \right]^{1/2}} \mathcal{E}^{1/2} + O(\mathcal{E}^0). \quad (46)$$

In contrast to the previous case, the asymptotic limit is now approached from above. Moreover, the analytical form has changed, since Eq. (46) indicates a series in powers of  $\mathcal{E}^{1/2}$ .

The dependence of the neutron star masses on  $\xi$  follows the same trend as found for  $\zeta$ . This can be gleaned from Fig. 6, which shows results for pure neutron matter. For fixed  $\zeta$ , the maximum mass decreases with increasing  $\xi$ , although the effect of this new parameter is smaller (less than a 10% change in the maximum mass), given the limitation on parameter values imposed by naturalness.

A more complete picture of  $M_{\max}$  is given in Fig. 7, where the variations with both  $\zeta$  and  $\xi$  are shown. It is apparent that parameter sets that yield identical properties near nuclear equilibrium can still generate values of the maximum mass that differ by as much as one solar mass. We find variations between  $M_{\max} = 2.9 M_\odot$  and  $M_{\max} = 1.9 M_\odot$  for stars composed of pure neutron matter. The masses are most sensitive to changes at small values of the couplings, particularly for  $\zeta \approx 0$ , which can be related to the nonanalytic form of the EOS in terms of  $\zeta$  and  $\xi$ . [See Eqs. (44)–(46).] As seen earlier, the effect of  $\xi$  is smaller than that of  $\zeta$ .

So far, we have considered pure neutron matter, which gives only a qualitative picture of neutron star properties. For a more realistic description, it is necessary to consider beta-stable matter, as this includes the protons, which softens the EOS. Maximum neutron star masses for beta-stable matter are also shown in Fig. 7. The dependence on the isoscalar coupling  $\zeta$  is similar to that obtained earlier (the maximum mass varies between  $M_{\max} = 2.8 M_{\odot}$  and  $M_{\max} = 1.8 M_{\odot}$ ), but the influence of the isovector coupling  $\xi$  is less drastic, since the matter becomes significantly more symmetric in the region that gives the largest contribution to the mass.

In Fig. 8, we examine the dependence of the maximum mass on the compression modulus at equilibrium, which is not particularly well known. (Relativistic mean-field models with  $200 \lesssim K_0 \lesssim 350$  MeV can produce accurate nuclear binding-energy systematics and surface energetics [21].) The shaded band shows the total predicted variation in maximum mass when both  $\zeta$  and  $\xi$  are varied within the bounds imposed by naturalness. The dashed curve shows the predicted variation when  $K_0$  is varied at fixed  $\zeta$  and  $\xi$ . Evidently, the variations in the maximum mass arising from the possibility of nonlinear vector meson interactions is much greater than that arising from the uncertainty in the compressibility.

These results raise the interesting question of whether the only significant nonlinearity is the quartic, isoscalar vector interaction. In other words, once one takes  $\zeta \neq 0$  to soften the EOS at high densities, does the addition of further nonlinearities produce only small effects? To examine this question, we extend the model of Eq. (38) to include sixth-order and eighth-order terms involving the vector-isoscalar meson:

$$\Delta\mathcal{V}' = -\frac{\zeta'}{6!}g_v^6(V_{\mu}V^{\mu})^3 - \frac{\zeta''}{8!}g_v^8(V_{\mu}V^{\mu})^4. \quad (47)$$

Thus  $\zeta'/6!$  and  $\zeta''/8!$  are the relevant ratios to be included in the parameter list given earlier, and we will initially set  $\xi$  to zero and examine the consequences of varying  $\zeta$ ,  $\zeta'$ , and  $\zeta''$  within the bounds imposed by naturalness.

Figure 9 shows neutron star masses as higher-order vector nonlinearities are included sequentially. Evidently, the quartic interactions are the most important, producing a roughly 30% variation in the maximum. The effects of the sixth-order term are quite modest (roughly 10%), while the eighth-order contributions are essentially negligible (roughly 2%). Here the parameters are varied within the natural ranges  $0 \leq \zeta \leq 0.06$ ,  $0 \leq \zeta' \leq 1.2$ , and  $0 \leq \zeta'' \leq 60$ . Thus we have the encouraging result that once the  $W^4$  interaction has been accurately calibrated, contributions from higher-order nonlinearities are relatively unimportant. To indicate the most extreme reduction in maximum mass possible in the present model, the cross in Fig. 9 shows  $M_{\max} = 1.58 M_{\odot}$ , which is obtained for *beta-stable matter* when the couplings  $\zeta = 0.06$ ,  $\zeta' = 1.2$ ,  $\zeta'' = 60$ , and  $\xi = 1.5$  are included. Note that this value of  $M_{\max}$  is only slightly ( $\approx 10\%$ ) larger than that of the most massive observed neutron stars.

Our analysis to this point has revealed significant model and parameter dependence in the high-density EOS. It is therefore of interest to see if these variations influence predictions arising from other relevant dynamics in systems with high densities. As an example, we study the effect of the high-density hadronic EOS on the existence of quark-matter cores in neutron stars. We adopt a simple two-phase model [37,1] based on a first-order (van der Waals) phase transition between the hadronic and quark phase. Although there are indications from QCD lattice calculations that the hadron/quark phase transition is second-order at vanishing chemical potential [50,51] (for massless quarks), the true behavior of the

transition at finite density (and indeed, whether one actually exists) is unknown at present. Until more reliable information is available, one must resort to a separate description of the quark phase and the hadronic phase. Moreover, whereas a detailed description involving beta-stable matter requires a careful treatment of the phase transition in systems with two conserved charges (baryon number and isospin) [27,49], here we will be satisfied with a qualitative discussion based on pure neutron matter. This is certainly reasonable, given the large uncertainties we have already found in the hadronic EOS at high density.

We adopt the simple EOS involving massless  $u$  and  $d$  quarks given by

$$p = \frac{1}{3}\mathcal{E} - \frac{4}{3}b, \quad (48)$$

where the confinement property of QCD (or alternatively, the anomaly in the trace of the energy-momentum tensor) is modeled by a positive constant  $b$ , which represents the energy per unit volume in the vacuum.

We return to the hadronic model of Eq. (38), which leads to the high-density expansion in Eq. (46). Our discussion is based on the simple observation that independent of the actual nature of the transition, it is driven purely by the energetics in the two phases.

By comparing Eq. (48) with the expansion in Eq. (46), one observes that in the quark phase, the limit  $p = \mathcal{E}/3$  is approached from below, whereas in neutron matter, for the general case  $\zeta > 0$  and  $\xi > 0$ , the limit is approached from above. To decide whether a transition takes place, it is necessary to compare the energy/baryon in both phases. For the quark phase it is expressed as [37]

$$\mathcal{E}/\rho = \frac{3}{4}\pi^{2/3}f(\alpha_s)\rho^{1/3} + b/\rho, \quad (49)$$

with

$$f(\alpha_s) = (1 + 2^{4/3})(1 + \frac{2\alpha_s}{3\pi}),$$

which includes the lowest-order contribution in  $\alpha_s$  (the exchange energy). As discussed in the preceding section, in hadronic models that are characterized by Eqs. (44) and (45), the quadratic terms dominate at high densities, so that

$$\lim_{\mathcal{E} \rightarrow \infty} \mathcal{E}/\rho \propto \rho, \quad (50)$$

for  $\zeta \geq 0$  and  $\xi = 0$ . This is also true if  $\zeta = 0$  and  $\xi \geq 0$ . Thus, at sufficiently high densities, neutron matter always has higher energy compared to the quark phase [37], and the two phases can be connected by a Maxwell construction, which signals the transition from hadron to quark matter.

The situation is different in the general case  $\zeta > 0$ ,  $\xi > 0$ . For the asymptotic form of the energy corresponding to Eq. (46), one obtains

$$\lim_{\mathcal{E} \rightarrow \infty} \mathcal{E}/\rho = \frac{3}{4}(3\pi^2)^{1/3} \left[ 1 + \left( \frac{2}{\pi^2 \zeta} \right)^{1/3} + \frac{1}{2} \left( \frac{1}{\pi^2 \xi} \right)^{1/3} \right] \rho^{1/3} + O(\rho^{-1/3}), \quad (51)$$

which is, up to the prefactor, the same leading behavior as in Eq. (49) for the quark phase. Therefore a phase transition is possible, *i.e.*, neutron matter has higher energy, only if

$$3^{1/3} \left[ 1 + \left( \frac{2}{\pi^2 \zeta} \right)^{1/3} + \frac{1}{2} \left( \frac{1}{\pi^2 \zeta} \right)^{1/3} \right] > f(\alpha_s) . \quad (52)$$

This remarkable observation implies that for sufficiently large values of the nonlinear couplings, the matter remains in the hadron (neutron) phase, at least in the simple model discussed here. More generally, one observes that independent of the asymptotic form, increasing the couplings  $\zeta$  and  $\xi$  increases the density at which the phase transition occurs (if it does), since the hadronic EOS becomes softer as the nonlinear couplings increase.

The different possibilities are illustrated in Fig. 10. The curve labeled *a* corresponds to Eq. (50); the asymptotic behavior is clearly different from the quark EOS. The phase transition occurs at roughly  $3\rho_0$ , and the Maxwell construction is indicated by the dotted line. In the situation described by curve *b*, neutron matter and quark matter have a similar asymptotic behavior, but the condition (52) remains true, and the two curves cross, leading to a phase transition at roughly  $6\rho_0$ . Finally, curve *c* lies completely below the quark EOS and a transition is not possible; neutron matter is stable at all densities.

If one introduces interaction terms of higher than fourth order in the fields, for example,  $(V_\mu V^\mu)^3$ , the hadronic energy is dominated by the Fermi gas contribution, and Eq. (51) must be replaced by

$$\lim_{\mathcal{E} \rightarrow \infty} \mathcal{E}/\rho = \frac{3}{4} (3\pi^2)^{1/3} \rho^{1/3} + O(\rho^{-1/3}) . \quad (53)$$

Since  $3^{1/3} < f(\alpha_s)$ , no transition is possible in the asymptotic regime for any choice of hadronic parameters in this case. On the other hand, the transition regime also depends on the model and parameters used for the description of the quark phase. In our model, the vacuum constant  $b$  and strong coupling  $\alpha_s$  can be used to shift the transition point substantially [52,53], so that a transition may occur outside the asymptotic regime. It is clear, however, that the strong model dependence in the hadronic EOS introduces large uncertainties in any attempted prediction of these values.

The consequences for neutron stars in this model follow straightforwardly. Nonlinear vector meson interactions soften the hadronic EOS, which lowers the maximum neutron star mass and increases the density of the transition to quark matter. In contrast, a stiff hadronic EOS lowers the density of the phase transition, and since the quark matter EOS is soft, also tends to decrease the maximum star mass. Thus it may be impossible to decide, from neutron star masses alone, whether quark matter cores exist in neutron stars, and similar conclusions may be drawn about other exotic phenomena that soften the EOS. (The situation is complicated further by the continuous nature of the transition when two conserved charges are involved, which is the more physical case [27].) Whereas it might be possible, using the results of more advanced calculations of the finite-density hadron/quark phase transition, to rule out certain parametrizations of the hadronic EOS, existing uncertainties in both the nature of the phase transition and in the high-density hadronic EOS preclude any definite conclusions at this time.

## V. SUMMARY

In this paper we study the equation of state of nuclear and neutron-star matter based on relativistic mean-field theory. Our starting point is an effective action (or energy functional)

containing Dirac nucleons and local scalar and vector fields. These fields are interpreted as relativistic Kohn–Sham potentials, and nonlinear interactions between the fields are introduced to parametrize the density dependence of the energy functional. We calibrate the energy functional by observing that at normal nuclear densities, the ratios of the mean fields to the nucleon mass are small, and thus the nonlinear interactions can be truncated at some low order in the fields. The unknown parameters can then be fit to properties of nuclear matter near equilibrium that are known to be characteristic of the observed bulk and single-particle properties of nuclei.

We then extrapolate the resulting equation of state into the neutron-rich, high-density regime to calculate the properties of neutron stars. Two problems arise in the extrapolation: First, even with a significant truncation of the energy functional, the unknown parameters are underdetermined. Thus there exist families of parameters that reproduce exactly the same nuclear matter properties near equilibrium, but which produce potentially different high-density equations of state. Second, terms omitted from the functional because they are negligible at normal density may become important at densities relevant for neutron stars. This is true even if we assume that the coupling parameters are “natural”, which means that they are all of roughly the same size when expressed in appropriate dimensionless ratios.

Our basic goal is to determine, in light of these two problems, whether the calibration at equilibrium nuclear matter density is sufficient to predict a maximum neutron star mass within a reasonably small range. This is relevant in view of recent calculations that hope to see evidence for “new” physics in neutron stars (such as quark cores, strange matter, or kaon condensates) based on the need for a softer high-density equation of state than that provided by neutrons, protons, and electrons alone. These calculations assume that the high-density behavior of these more mundane components is well known, and in particular, that the contributions of many-nucleon forces are negligible [27–32]. These many-body, density-dependent forces are precisely the ones that are difficult to calibrate using observed nuclear properties; the question is whether one can build nuclear equations of state with different types of many-body forces that all reproduce the observed properties near equilibrium, but which yield significantly different results at high density.

By beginning with a meson self-interaction potential containing arbitrary powers of scalar-isoscalar ( $\sigma$ ), vector-isoscalar ( $\omega$ ), and vector-isovector ( $\rho$ ) fields, we show that the meson nonlinearities can have a profound effect on the high-density equation of state. In models where the vector mesons enter the potential at most quadratically, the equation of state is stiff and asymptotically approaches  $p = \mathcal{E}$ . (The Walecka model is a special case.) In models where the vector fields enter with high powers, these fields become negligible at high density, and the asymptotic equation of state resembles that of a free, relativistic gas:  $p = \mathcal{E}/3$ . The intermediate case occurs when the vector fields enter quartically; the asymptotic equation of state is still soft ( $p = \mathcal{E}/3$ ), but the approach to the asymptotic limit is determined by the coupling parameters.

We illustrate these results using specific models containing quartic  $\omega$  and  $\rho$  meson couplings and also sixth- and eighth-order  $\omega$  couplings. All models are calibrated to exactly the same nuclear properties at equilibrium, for all choices of parameters. We find that by far the most important coupling constant is that of the quartic  $\omega$  term; even when restricted by the requirements of naturalness, variations in this parameter can produce variations of nearly one solar mass in the predicted maximum neutron star mass. (This is true for both

pure neutron matter and for beta-stable matter.) This uncertainty is clearly relevant on the scale on which one hopes to identify new, exotic effects. Moreover, increasing the strength of the quartic coupling softens the equation of state, which is precisely the effect sought from the exotica. The impact of a quartic  $\rho$  meson coupling is smaller, and its effects are only appreciable in stars made of pure neutron matter; the maximum masses of stars computed with beta-stable matter show little change when this parameter is varied within the bounds imposed by naturalness. Similarly, sixth-order  $\omega$  interactions have only a modest effect on the predicted maximum mass, and by the time the eighth-order terms are included, the high-density equation of state is already so soft that these terms are negligible.

We emphasize that the importance of these many-body effects is not limited to the domain of relativistic mean-field theories; equations of state based on nonrelativistic potentials [26] use interactions that are calibrated to few-body systems and that are insensitive to possible six- or eight-body forces that may be relevant at high density. This is especially important because a mean-field calculation with four-component spinors and just *two-body* Lorentz scalar forces already implicitly contains an infinite string of many-body forces if it is recast in terms of two-component spinors.

To illustrate these difficulties more concretely, we also study the role of the hadron/quark phase transition in a simple two-phase model with a first-order transition. We find that with couplings well within the bounds of naturalness, it is possible to push the phase transition to arbitrarily high density, and even to make it disappear altogether. Although the absence of a phase transition is probably unrealistic and could serve to exclude some values of the hadronic parameters, there are still too many uncertainties on both sides of the transition (as well as in the nature of the transition itself!) to make any definitive statements.

We therefore conclude that existing methods for calibrating the nuclear equation of state for extrapolation into the neutron-rich, high-density regime appropriate for neutron stars cannot constrain the predicted maximum star mass well enough to make reliable statements about the existence of “new” physics beyond the dynamics of neutrons, protons, and electrons. We show that the uncertainties arising from an incomplete knowledge of the hadronic many-body forces are much larger than those arising from an imperfect knowledge of the properties of nuclear matter near equilibrium, such as the nuclear matter compression modulus. Even the old question of the role of the hadron/quark phase transition is problematic, since the high-density hadronic equation of state can be made essentially as soft as desired by the addition of nonlinear interactions that are still consistent with equilibrium nuclear matter properties.

One positive conclusion is that the most important nonlinear parameter is that of the quartic  $\omega$  interaction. If this term could be accurately calibrated, the uncertainties introduced by other nonlinear interactions are likely to be tolerable. (One caveat: we do not study carefully the sensitivity to variations in mixed scalar–vector interactions because of the overwhelming sensitivity to the quartic  $\omega$  term; if the latter were well constrained, the role of scalar–vector interactions should be examined in more detail.) Although this coupling has not been extensively studied in mean-field calculations, there are several possibilities for determining it reasonably well. First, since a quartic  $\omega$  interaction leads to a nonlinear density dependence in the vector part of the baryon self-energy, one could calibrate this interaction by fitting to the self-energy obtained in a Dirac–Brueckner–Hartree–Fock calculation, for example. Although some initial attempts at this procedure have been made [20],

the resulting parameters are not always natural; it is probably necessary to repeat the procedure using all possible scalar and vector self-interactions through fourth order and to fit both the scalar and vector part of the self-energy simultaneously. Second, the nonlinearities in the energy functional can be interpreted in terms of effective masses for the vector and scalar mesons (defined by diagonalizing the matrix of appropriate second derivatives of the energy functional). This may provide useful constraints in the future, if concrete empirical information on these effective masses becomes available. Third, it is possible that additional observables in finite nuclei could constrain the nonlinear interactions. For example, some recent work suggests that the ratio of the nuclear matter “skewness” (which is related to the third derivative of the energy with respect to density at equilibrium) to the compression modulus  $K$  is constrained by monopole vibrations. Although a recent calculation of nuclear ground-state properties shows little correlation with this ratio [21], a more detailed examination of dynamical effects could provide meaningful constraints.

To summarize, precise predictions of the properties of neutron stars apparently require more accurate calibrations of the nuclear equation of state than are currently available. It is especially important to have the high-density behavior of the “standard” components (neutrons, protons, and electrons) under control before one can make reliable statements about the existence of “new” physics. Since the window on experimentally observable nuclear properties is a narrow one, producing an equation of state that can be extrapolated with confidence remains a major challenge.

#### ACKNOWLEDGMENTS

We thank R. J. Furnstahl and H.-B. Tang for useful comments. This work was supported in part by the Department of Energy under Contract No. DE-FG02-87ER40365.

## REFERENCES

- [1] B. D. Serot and J. D. Walecka, *Adv. Nucl. Phys.* 16 (1986) 1.
- [2] B. D. Serot, *Rep. Prog. Phys.* 55 (1992) 1855.
- [3] J. D. Walecka, *Ann. Phys. (N.Y.)* 83 (1974) 491.
- [4] J. Boguta and A. R. Bodmer, *Nucl. Phys. A* 292 (1977) 413.
- [5] B. D. Serot, *Phys. Lett.* 86 B (1979) 146; 87 B (1979) 403 (E).
- [6] P. G. Reinhard, M. Rufa, J. Maruhn, W. Greiner, and J. Friedrich, *Z. Phys. A* 323 (1986) 13.
- [7] R. J. Furnstahl, C. E. Price, and G. E. Walker, *Phys. Rev. C* 36 (1987) 2590.
- [8] R. J. Furnstahl and C. E. Price, *Phys. Rev. C* 40 (1989) 1398.
- [9] A. R. Bodmer and C. E. Price, *Nucl. Phys. A* 505 (1989) 123.
- [10] Y. K. Gambhir, P. Ring, and A. Thimet, *Ann. Phys. (N.Y.)* 198 (1990) 132.
- [11] R. J. Furnstahl and B. D. Serot, *Phys. Rev. C* 47 (1993) 2338.
- [12] D. G. Boulware, *Ann. Phys. (N.Y.)* 56 (1970) 140.
- [13] S. Weinberg, *Phys. Rev.* 166 (1968) 1568; *Physica A* 96 (1979) 327.
- [14] R. Dashen and M. Weinstein, *Phys. Rev.* 183 (1969) 1261.
- [15] J. Gasser and H. Leutwyler, *Ann. Phys. (N.Y.)* 158 (1984) 142; *Nucl. Phys. B* 250 (1985) 465, 517, 539.
- [16] H. Leutwyler, *Ann. Phys. (N.Y.)* 235 (1994) 165.
- [17] J. L. Friar, D. G. Madland, and B. W. Lynn, "QCD Scales in Finite Nuclei," preprint *nucl-th/9512011* (December, 1995).
- [18] R. J. Furnstahl, B. D. Serot, and H.-B. Tang, in preparation.
- [19] A. R. Bodmer, *Nucl. Phys. A* 526 (1991) 703.
- [20] S. Gmuca, *Z. Phys. A* 342 (1992) 387; *Nucl. Phys. A* 547 (1992) 447.
- [21] R. J. Furnstahl, B. D. Serot, and H.-B. Tang, *Nucl. Phys. A* 598 (1996) 539.
- [22] R. M. Dreizler and E. K. U. Gross, *Density functional theory* (Springer, Berlin, 1990).
- [23] C. Speicher, R. M. Dreizler, and E. Engel, *Ann. Phys. (N.Y.)* 213 (1992) 312.
- [24] R. N. Schmid, E. Engel, and R. M. Dreizler, *Phys. Rev. C* 52 (1995) 164.
- [25] W. Kohn and L. J. Sham, *Phys. Rev. A* 140 (1965) 1133.
- [26] B. Friedman and V. R. Pandharipande, *Nucl. Phys. A* 361 (1981) 502.
- [27] N. K. Glendenning, *Phys. Rev. D* 46 (1992) 1274.
- [28] T. Maruyama, H. Fujii, T. Moto, T. Tatsumi, *Phys. Lett. B* 337 (1994) 19.
- [29] R. Knorren, M. Prakash, and P. J. Ellis, *Phys. Rev. C* 52 (1995) 3470.
- [30] M. Prakash, J. Cooke, and J. M. Lattimer, *Phys. Rev. D* 52 (1995) 661.
- [31] M. Prakash, I. Bombaci, M. Prakash, P. J. Ellis, J. M. Lattimer, and R. Knorren, *Phys. Reports* (in press).
- [32] H. Fujii, T. Maruyama, T. Moto, and T. Tatsumi, Kyoto University preprint KUNS-1348 (1995).
- [33] G. Velo and D. Zwanzinger, *Phys. Rev.* 188 (1969) 2218.
- [34] G. Velo, *Nucl. Phys. B* 65 (1973) 427.
- [35] V. I. Ogievetskij and I. V. Polubarinov, *Ann. Phys. (N.Y.)* 25 (1963) 358.
- [36] J. C. Collins and M. J. Perry, *Phys. Rev. Lett.* 34 (1975) 1353.
- [37] G. Baym and S. A. Chin, *Phys. Lett.* 62 B (1976) 241.
- [38] N. K. Glendenning, *Ap. J.* 293 (1985) 470; *Nucl. Phys. A* 493 (1989) 521.
- [39] J. Ellis, J. I. Kapusta, and K. A. Olive, *Nucl. Phys. B* 348 (1991) 345.

- [40] H. D. Politzer and M. B. Wise, Phys. Lett. B 273 (1991) 156.
- [41] A. L. Fetter and J. D. Walecka, *Quantum theory of many-particle systems* (McGraw–Hill, New York, 1971).
- [42] C. Itzykson and J. B. Zuber, *Quantum field theory* (McGraw–Hill, New York, 1980) sec. 11–4–2.
- [43] J. Iliopoulos, C. Itzykson, and A. Martin, Rev. Mod. Phys. 47 (1975) 165.
- [44] R. J. Furnstahl, H.-B. Tang, and B. D. Serot, Phys. Rev. C 52 (1995) 1368.
- [45] C. J. Horowitz and B. D. Serot, Nucl. Phys. A 399 (1983) 529; A 464 (1987) 613; A 473 (1987) 760 (E).
- [46] H. Georgi, *Weak interactions and modern particle theory* (Benjamin/Cummings, Menlo Park, CA, 1984).
- [47] E. K. Heide, S. Rudaz, and P. J. Ellis, Nucl. Phys. A 571 (1994) 713.
- [48] W. D. Myers and W. J. Swiatecki, preprint LBL–36557 (1995).
- [49] H. Müller and B. D. Serot, Phys. Rev. C 52 (1995) 2072.
- [50] F. R. Brown, F. P. Butler, H. Chen, N. H. Christ, Z. Dong, W. Schaffer, L. I. Unger, and A. Vaccarino, Phys. Rev. Lett. 65 (1990) 2491.
- [51] N. H. Christ, Nucl. Phys. A 544 (1992) 81c.
- [52] B. D. Serot and H. Uechi, Ann. Phys. (N.Y.) 179 (1987) 272.
- [53] H. A. Bethe, G. E. Brown, and J. Cooperstein, Nucl. Phys. A 462 (1987) 791.

## FIGURE CAPTIONS

FIG. 1. Binding energy of symmetric and neutron matter.

FIG. 2. Equation of state of neutron matter.

FIG. 3. Neutron star masses for different nonlinear couplings  $\zeta$ . Pure neutron matter is assumed.

FIG. 4. Density distributions of neutron stars as a function of the radius, calculated with different parameters  $\zeta$ . The central mass density  $\rho_c = 1.5 \times 10^{15}$  g/cm<sup>3</sup> is the same for all curves. Part (a) shows the radial mass densities and part (b) the corresponding energy densities. The stars acquire most of their mass from the region  $100 \lesssim \mathcal{E} \lesssim 500$  MeV/fm<sup>3</sup>.

FIG. 5. Energy difference  $\Delta\mathcal{E} = [\mathcal{E}(\xi = 0) - \mathcal{E}(\xi)]/\mathcal{E}(\xi = 0)$  of nuclear matter as a function of the proton fraction  $y$  calculated at constant baryon density. In part (a) the density is fixed at its equilibrium value  $\rho_0$  and part (b) shows the results at  $5\rho_0$ . Note the different vertical scales in (a) and (b).

FIG. 6. Neutron star mass for different values of  $\xi$  at fixed  $\zeta$ . Pure neutron matter is assumed.

FIG. 7. Maximum neutron star mass as function of  $\zeta$  and  $\xi$ . Results for pure neutron matter and for matter in  $\beta$ -equilibrium are displayed. The shaded areas show the mass range obtained when  $\xi$  is varied; the upper boundaries correspond to  $\xi = 0$  and the lower boundaries to  $\xi = 1.5$ .

FIG. 8. Maximum neutron star mass as a function of the compression modulus  $K_0$ . (All other nuclear matter inputs are held fixed.) The shaded area marks the covered range of masses. The upper boundary corresponds to  $\zeta = 0, \xi = 0$  and the lower boundary to  $\zeta = 0.06, \xi = 1.5$ . For fixed values of the nonlinear couplings, the mass changes marginally with the compression modulus. This can be seen from the dashed line inside the shaded area, which corresponds to  $\zeta = 0.02, \xi = 0.5$ .

FIG. 9. Neutron star masses for models with different nonlinear couplings for the neutral vector meson. The uppermost curve corresponds to the Walecka model, including cubic and quartic couplings for the scalar meson. Region *A* shows the range of masses obtained when the quartic vector coupling is turned on. Regions *A* and *B* correspond to models with up to sixth-order terms, and regions *A*, *B*, and *C* include an eighth-order term. The values of the nonlinear couplings are chosen within a natural range, as described in the text. The cross indicates the maximum mass ( $1.58 M_\odot$ ) obtained for beta-stable matter in a calculation that includes the  $\zeta, \zeta', \zeta'',$  and  $\xi$  couplings (see the text).

FIG. 10. Energy per baryon for neutron matter (solid) and quark matter (dashed). The quark matter results are calculated using  $b = 120$  MeV/fm $^3$  and  $\alpha_s = 0.4$  [52].

## TABLES

TABLE I. Equilibrium Properties of Nuclear Matter

$(k_F)_0$	$\rho_0$	$M_0^*/M$	$e_0$	$K_0$	$a_4$
1.30 fm $^{-1}$	0.1484 fm $^{-3}$	0.60	-15.75 MeV	250 MeV	35 MeV

## FIGURES

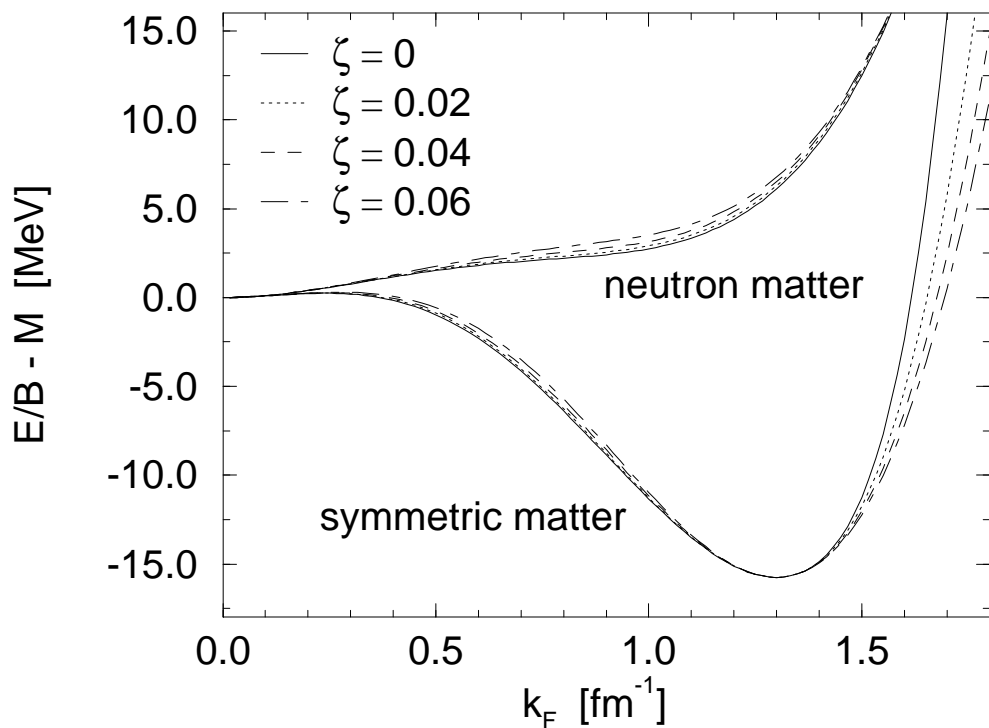


FIGURE 1

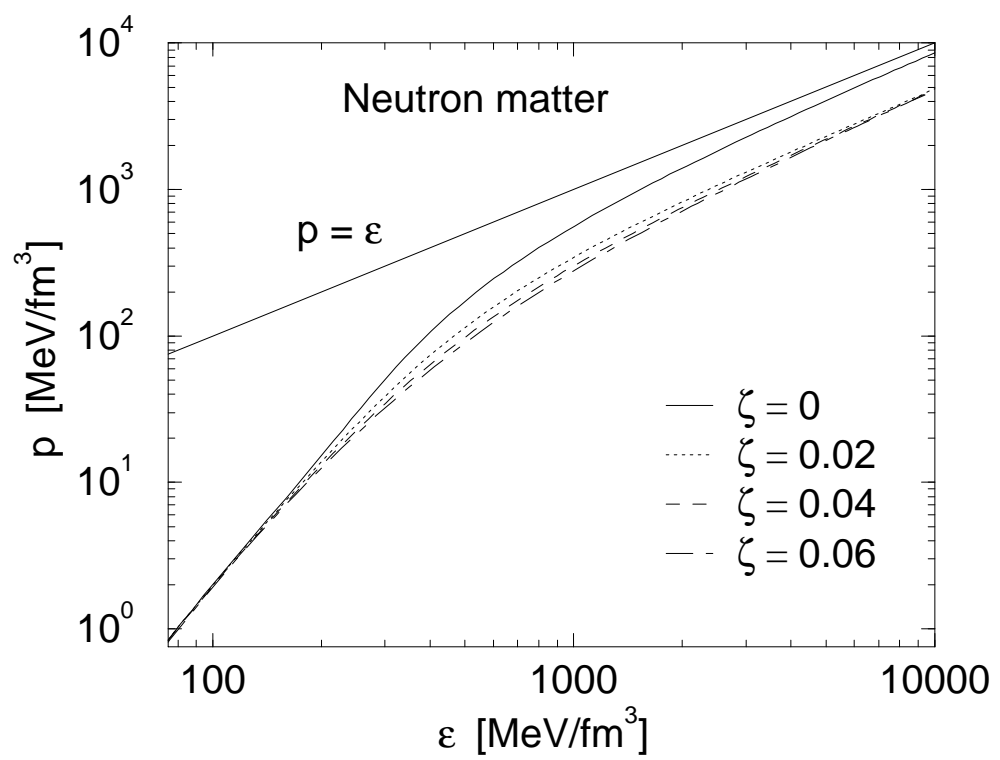


FIGURE 2

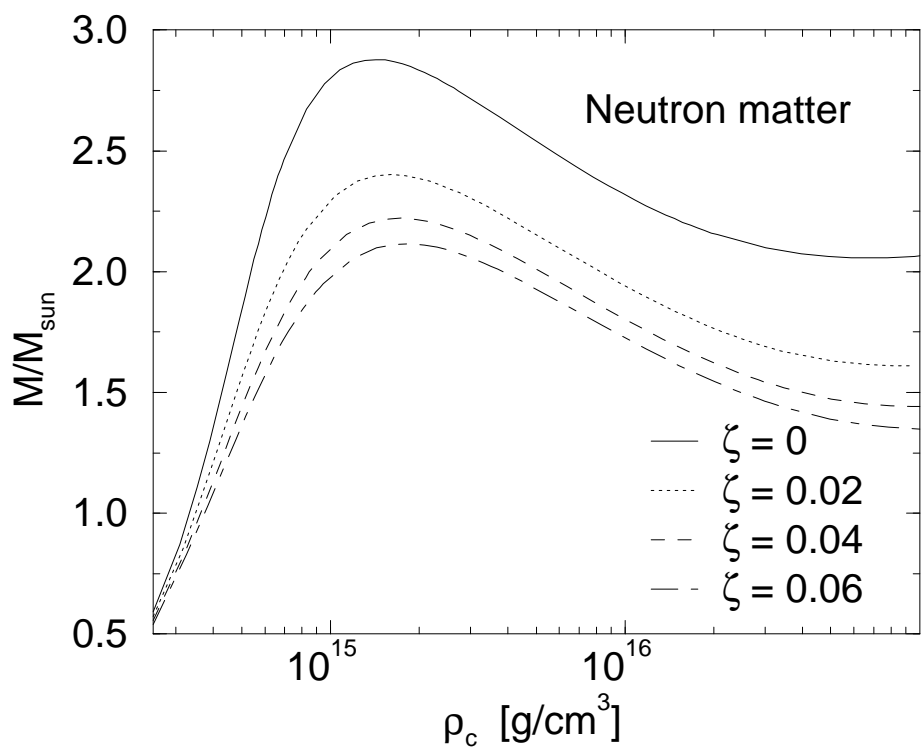


FIGURE 3

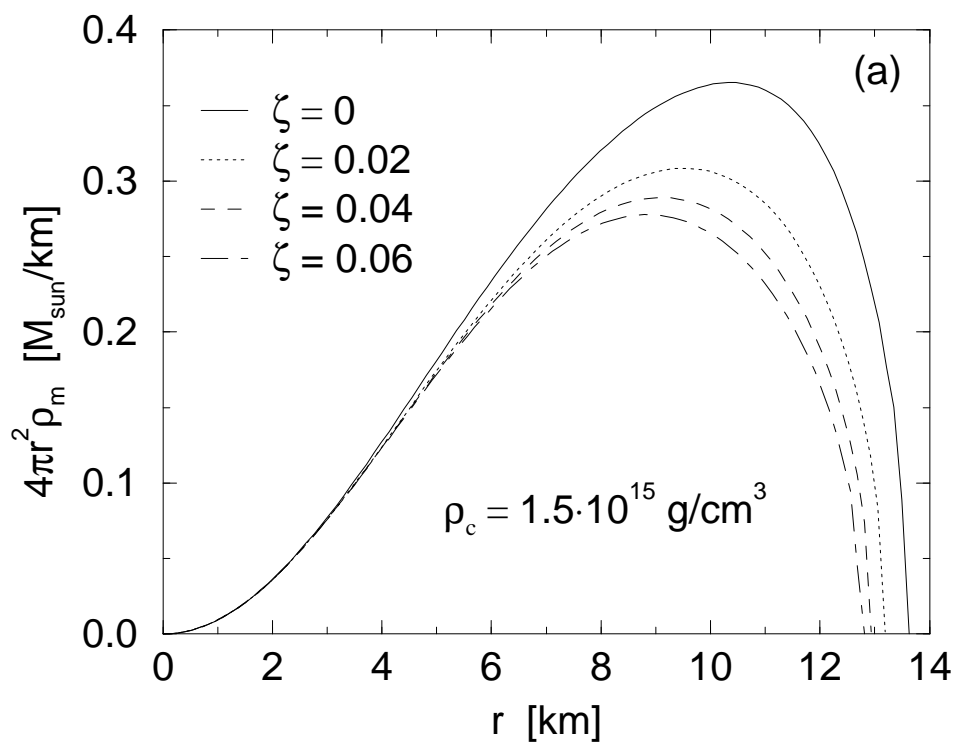


FIGURE 4(a)

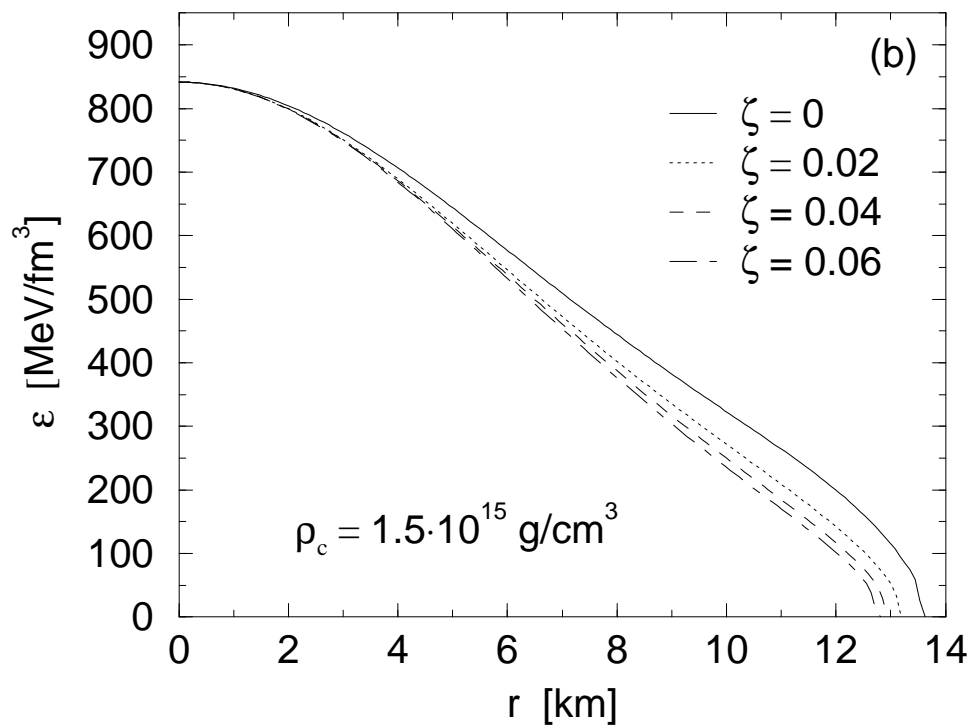


FIGURE 4(b)

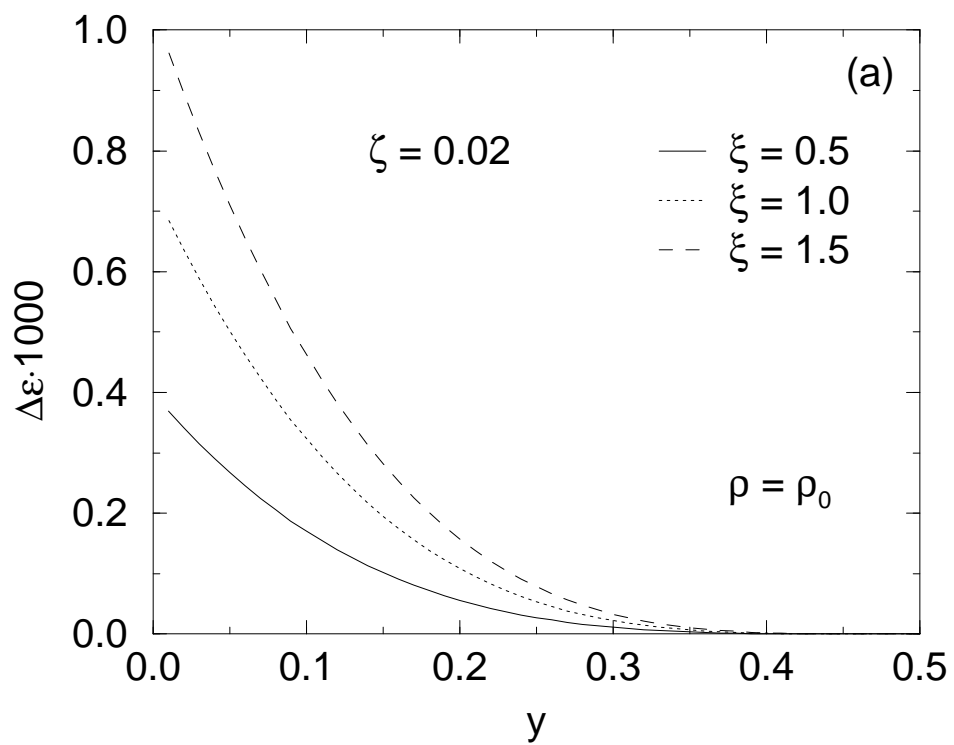


FIGURE 5(a)

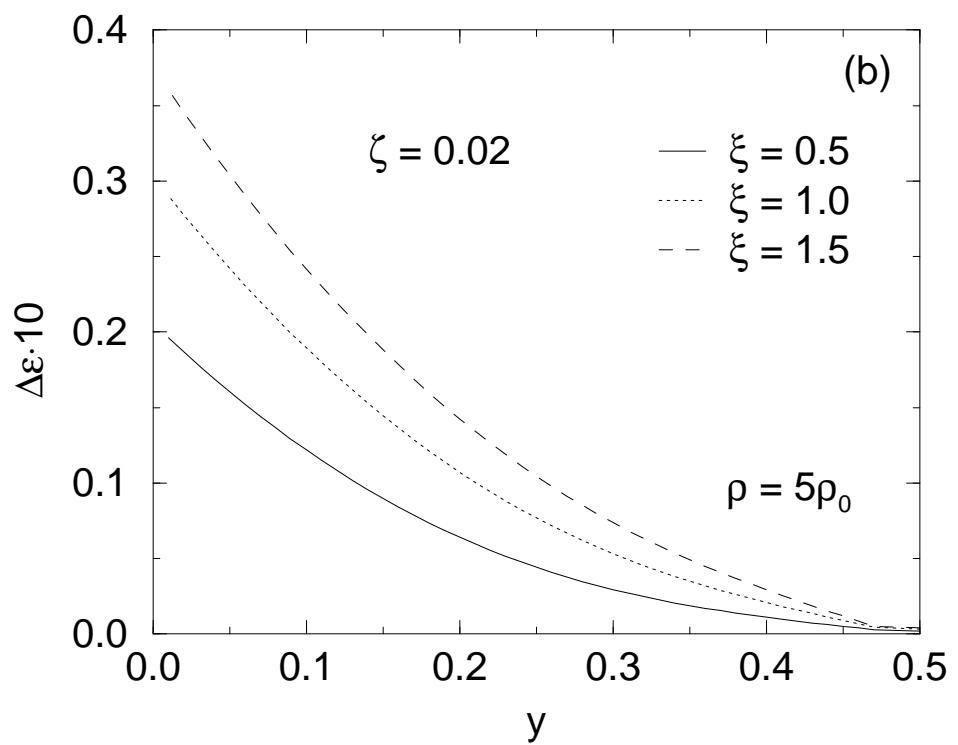


FIGURE 5(b)

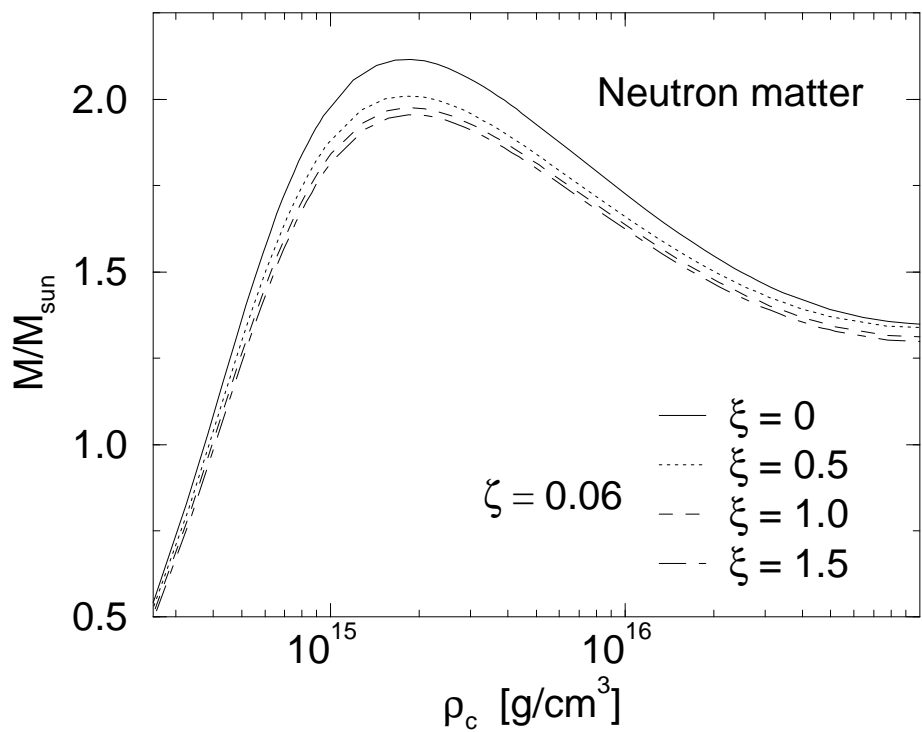


FIGURE 6

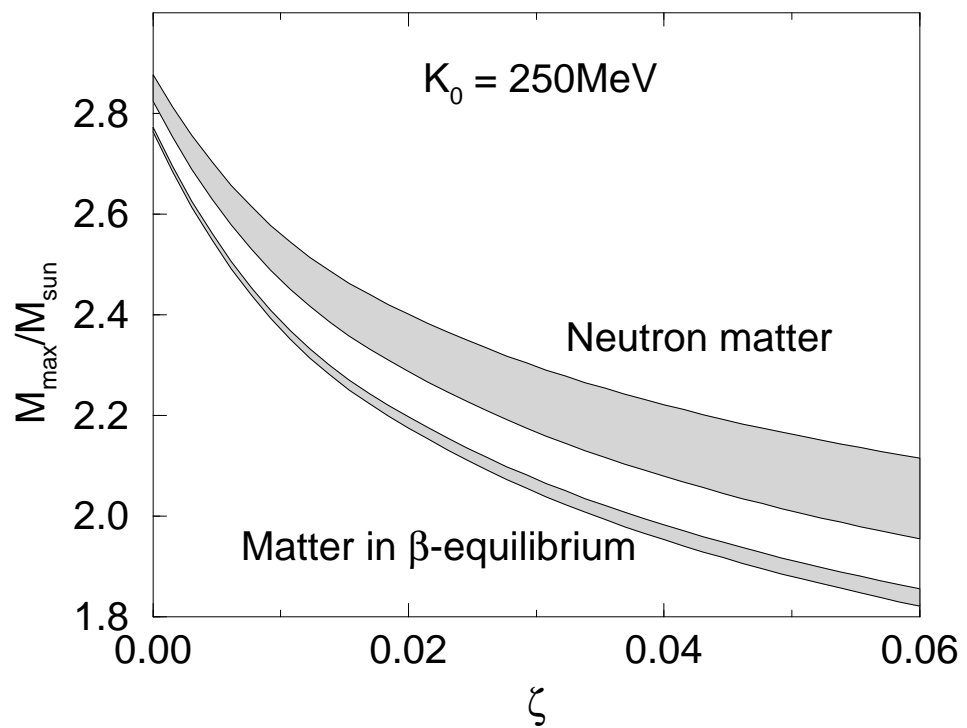


FIGURE 7

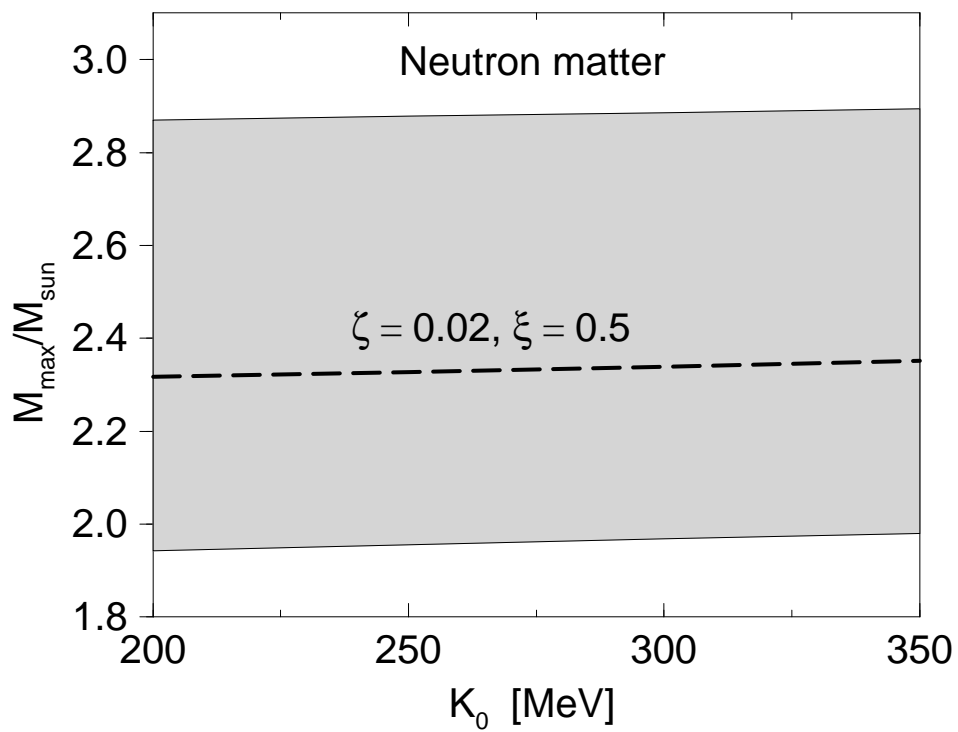


FIGURE 8

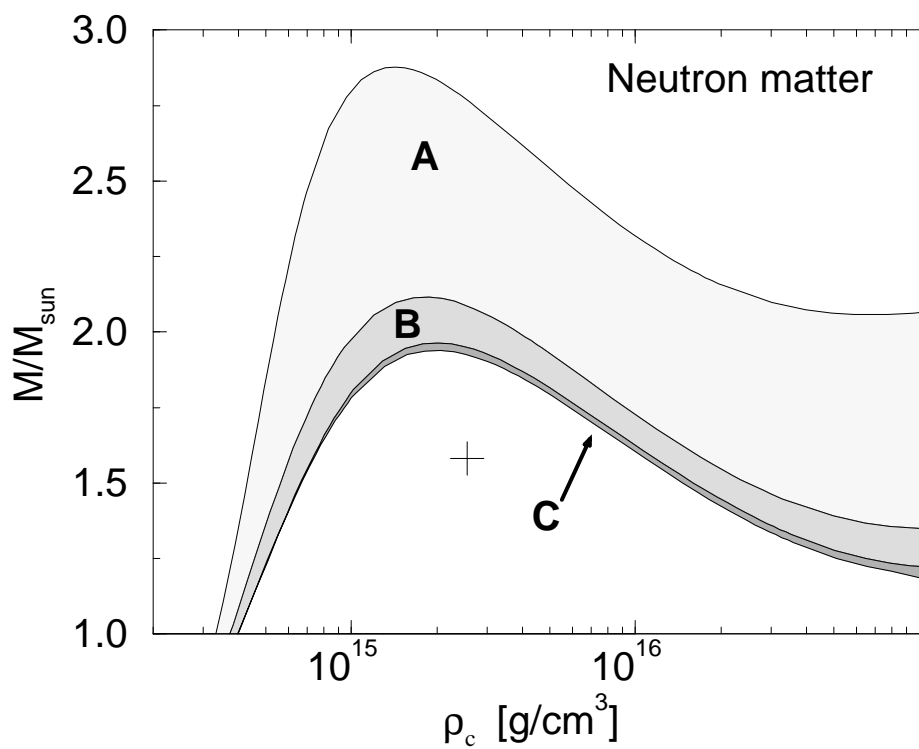


FIGURE 9

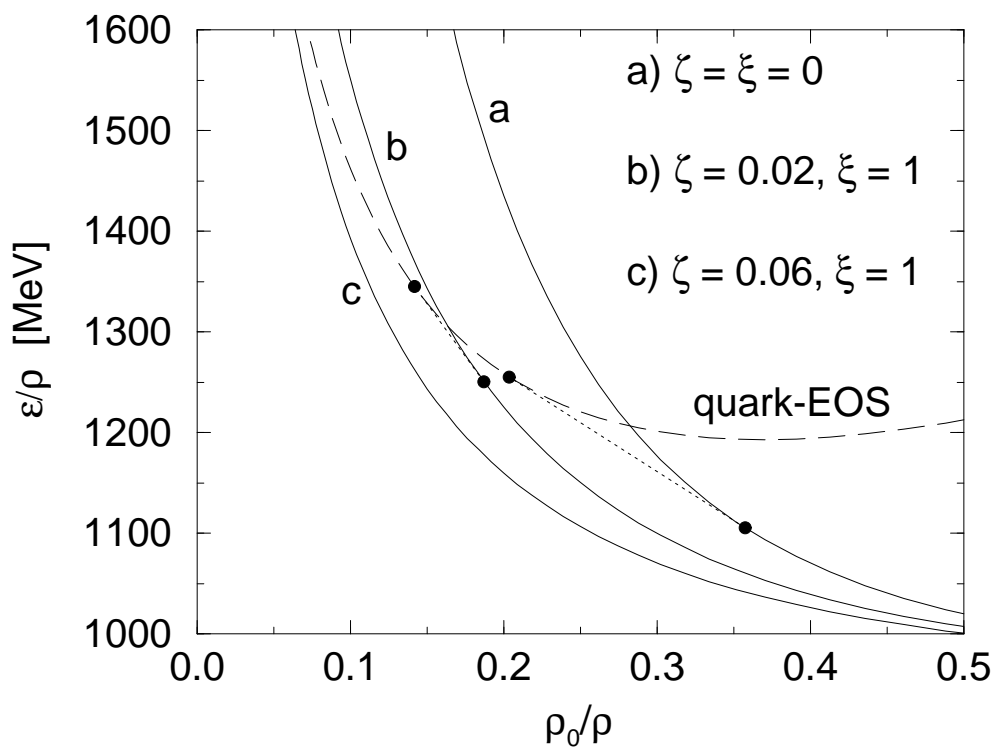


FIGURE 10